

## Manufacturing and Characterization of Corrosion Resistant Epoxy/2Pack Coatings Incorporated with Polyaniline Conductive Polymer

Ubair Abdus Samad<sup>1,2</sup>, Mohammad Asif Alam<sup>2</sup>, El-Sayed M. Sherif<sup>2,3,\*</sup>, Othman Alothman<sup>1,4</sup>, Asiful H. Sheikh<sup>2</sup> and Saeed Al-Zahrani<sup>2,5</sup>

<sup>1</sup> Chemical Engineering Department, College of Engineering, King Saud University, Riyadh 11421, Saudi Arabia

<sup>2</sup> Center of Excellence for Research in Engineering Materials (CEREM), Advanced Manufacturing Institute (AMI), King Saud University, P. O. Box 800, Al-Riyadh 11421, Saudi Arabia

<sup>3</sup> Electrochemistry and Corrosion Laboratory, Department of Physical Chemistry, National Research Centre (NRC), Dokki, 12622 Cairo, Egypt

<sup>4</sup> Deanship of Graduate Studies, The Saudi Electronic University, Riyadh 11673, Saudi Arabia

<sup>5</sup> SABIC Polymer Research Center (SPRC), Department of Chemical Engineering, College of Engineering, King Saud University, P.O. Box 800, Al-Riyadh 11421, Saudi Arabia

\*E-mail: [esharif@ksu.edu.sa](mailto:esharif@ksu.edu.sa); [emsherif@gmail.com](mailto:emsherif@gmail.com)

Received: 6 April 2015 / Accepted: 15 May 2015 / Published: 27 May 2015

---

Different epoxy coatings incorporated with different additions of up to 0.78 wt. % polyaniline (PANI) were manufactured. The dispersion of PANI with epoxy was done using both mechanical and sonication processes. The surface of the fabricated coatings was characterized using field emission scanning electron microscopy (FE-SEM). The chemical composition was also confirmed by using Fourier transform infrared (FTIR-ATR). The hardness, scratch resistance, impact strength, load vs. depth using nanoindentation, and thermal degradation for all of the manufactured coatings were evaluated. The corrosion resistance of the PANI modified coatings after different immersion periods of time, namely, 1 h, 7 days, and 21 days in 3.5 wt. % NaCl solutions were reported using electrochemical impedance spectroscopy (EIS) measurements. Measurements proved that these coatings have excellent mechanical properties and provide good corrosion protection, which is superior as compared to conventional epoxy coatings. Results also indicated that PANI can be considered as suitable alternative to replace hazardous inorganic anticorrosive pigments currently used in coating formulations.

---

**Keywords:** conducting polymers; corrosion; EIS; epoxy coatings; nanoindentation; scratch resistance

## 1. INTRODUCTION

Epoxy coatings are being applied on numerous substrates to protect it against corrosion because of their excellent adhesion, high performance mechanical properties as well as chemical resistance in various harsh conditions and aggressive environments. They are being used in heavy machineries industries, coastal areas, and in wet and humid surfaces of different types of substrates. The epoxy coatings which are generally applied with epoxy zinc rich primer may face a failure due to the prolonged exposure to these humid and wet areas, where the environmental degradation takes place at these coated substrates for various reasons. The applied coating can develop corrosion failure that starts from weak areas leading to the formation of blisters causing a partial or complete damage to substrate coated with epoxy primer. The reason of the failure of the epoxy coating system occurs due to the separation process known as delaminating of the coated film at the coating/metal interface. Different types of corrosion inhibiting pigments have been used in epoxy coating formulations and primers such as zinc phosphate, lead chromates, strontium chromates, and metaborates, which are used in huge quantity and are the reason of environmental hazard. In order to overcome the problems of these inhibiting pigments and failure of the coating, different types of conducting polymers such as poly-aniline and poly-thiophene can be incorporated along with epoxy coating formulations to obtain a high performance corrosion resistance, chemical resistance, and low dry film thickness coating for petroleum industries application.

Oil and gas pipelines suffer both internal and external corrosion due to the corrosivity of the surrounding media. This corrosion if takes place will cause the destruction of the pipeline and therefore the leaking of the transported oil and/or gas. This effect can also cause the rupture of the storage tanks, which in most cases results in a big loss of human lives, energy, time, and materials to replace the destroyed pipelines and tanks. The use of protective coatings corrosion can be considered as one of the most important ways to prevent the corrosion of metals and alloys. Conducting polymers (CPs) have been widely employed in several applications [1-5]. Some of these applications are in the protection of metals and alloys against corrosion in harsh media [4-6]. The trials in the use of protective coatings were started by DeBerry [1] and Mengoli et al. [3]. Extensive research work has been continued in order to find a substitute for the toxic chromium (VI)-containing coatings for controlling the corrosion of metals and alloys. CPs coatings containing poly-pyrrole (PPy) or poly-aniline (PANI) have been reported to be good replacements for the toxic chromium (VI)-containing coatings as a result of their high conductivity and good reduction-oxidation properties.

The recent trends in the use of environmentally friendly protective coatings led to the use of the conducting polymers incorporated within the coatings [7-10]. Lu et al. [10] have stated that the electroactive polymers, like PANI and PPy, show good corrosion protection to mild steel in various corrosive media. The PANI and PPy have been reported as good alternatives to chromate conversion coatings and as anti-corrosion coatings [11]. In this study, intention of the authors was to manufacture different coatings containing conducting polymer to replace the conventional and toxic epoxy coatings. In order to achieve this objective, different epoxy coatings incorporated with different wt. %s of PANI using both mechanical and sonication methods and evaluating their mechanical properties and corrosion resistance were reported. The mechanical properties were investigated using various

mechanical testing techniques. The corrosion resistances of the different coatings after being exposed to 3.5 wt. % NaCl solutions for 0, 7, and 21 days were also reported. It is believed that the higher solubility of PANI as a conducting polymer in the epoxy coating will allow other investigators to extensively study these compounds in the field of corrosion protection.

## 2. EXPERIMENTAL SETUP

### 2.1. Materials

Epoxy coatings formulations (EPANI1- EPANI4) were prepared by the reaction between bisphenol-A diglycidyl ether epoxy resin (DGEBA) as the epoxy resin (Hexion Chemicals) and polyamidoamine adduct as the hardener (Huntsman Advanced Materials). Different types of solvents and diluents, which facilitate the homogeneous mixing and compatibility of the formulations and are essential ingredients, were arranged from local companies in Saudi Arabia. The specific conductive polymer has been used for the preparation of coating formulations was polyaniline emeraldine salt, long chain, grafted to lignin (Cat. No.-561134) purchased from Sigma-Aldrich. Solvents used are xylene, methyl isobutyl ketone (MIBK), and acetone.

### 2.2. Manufacturing of epoxy coatings

**Table 1.** Incorporation of polyaniline in optimized epoxy/2pack formulations

Sample	Epoxy resin wt. %	PANI wt. %	Xylene	MIBK	Dispersing agent	Hardener D-3282 wt. %
EPANI1	82.91	0.16	20	20	1	16.57
EPANI2	82.08	0.25	20	20	1	16.41
EPANI3	79.58	0.63	20	20	1	15.91
EPANI4	78.33	0.78	20	20	1	15.66

The epoxy/2pack coatings were formulated by mixing a stoichiometric amount of epikote 1001 resin and an optimized quantity of polyamidoamine adduct hardener (D-3282). In addition, four different coating formulations of PANI–epoxy resin were prepared by mechanical mixing followed by sonication technique utilizing ultrasonic water bath. A mixture of alcoholic solvents and aromatic hydrocarbons was used for homogeneous dispersion and to reduce the viscosity of the formulations. Polyaniline in different percentages was added to dilute epoxy resin and mixed using mechanical stirrer (Sheen S2 disperse master) for 1 h. The sonication was performed for 60 minutes at 50 °C after mixing of PANI in the epoxy resin. After complete mixing, the hardener was added in a stoichiometric amount to the formulation. Little amount of the solvent was also added into the prepared formulations to obtain homogeneous slurry and to reduce the viscosity. Table 1 shows typical percentages to formulation ingredients with stoichiometric amount of epoxy resin, hardener and the incorporated PANI conductive polymer.

### 2.3. Characterization of polyaniline incorporated epoxy /2pack coating:

The surface morphology of the coating samples and polyaniline powder were investigated via field emission scanning electron microscopy (FE-SEM). The FE-SEM investigation was performed using a JEOL JSM-7400F. The samples were mounted on a double-sided carbon tape and then were sputter coated with platinum to avoid any charging. Spectroscopic analysis of coating films has been carried out with Thermo Scientific FTIR spectrometer (model Nicolet IN10) using universal sampling accessory. Cross linking reactions at fixed stoichiometric mixture of epoxy resin with hardener & incorporation of conducting polymers were studied by using ATR-IR spectroscopy.

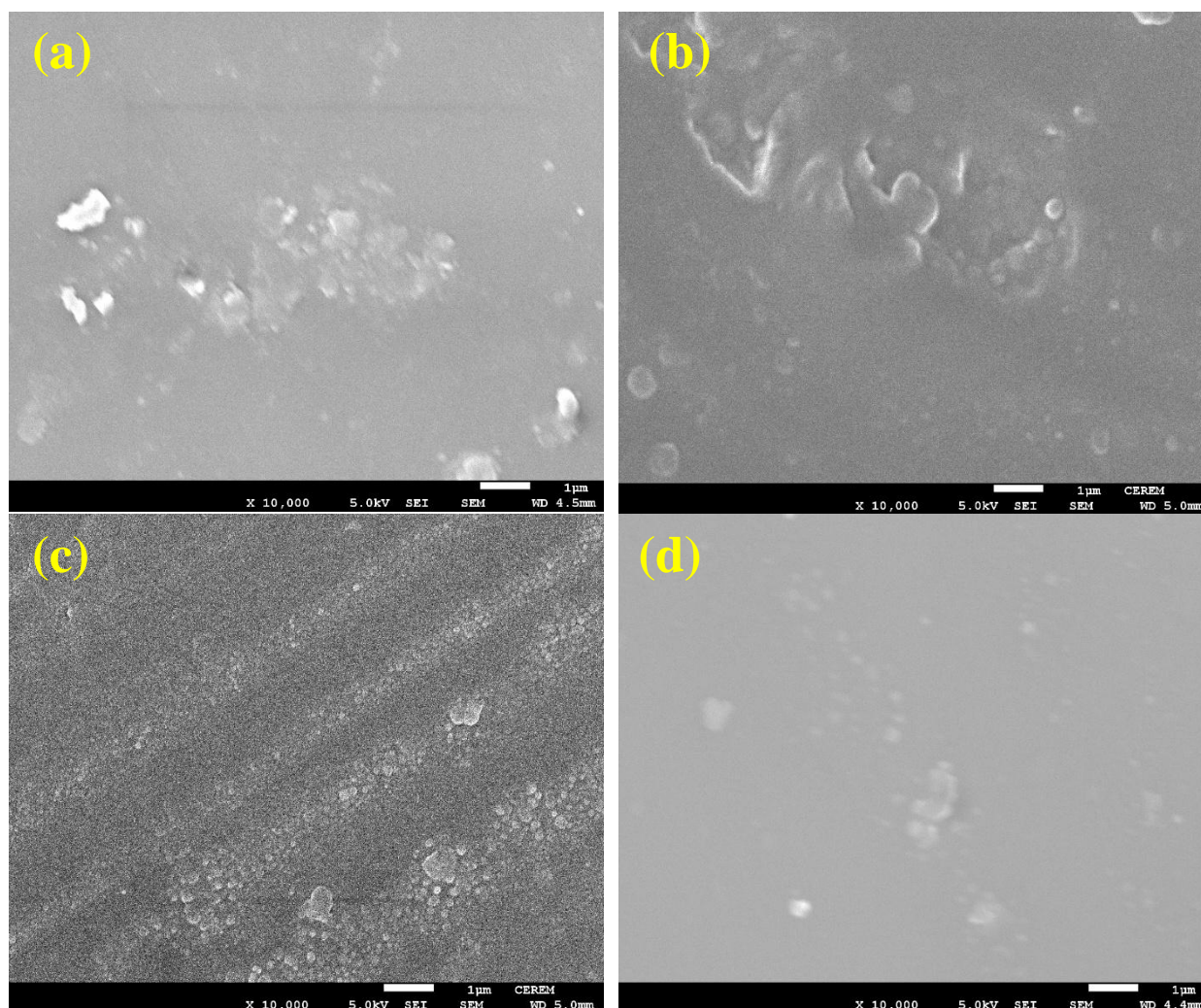


**Figure 1.** FE-SEM images of PANI modified epoxy coatings with (a) 0.16 wt. % PANI (b) 0.25 wt. % PANI (c) 0.63 wt. % PANI and (e) 0.78 wt. % PANI, respectively.

Hardness of coating samples was measured using Koenig pendulum tester (model 707/K) from Sheen Instruments following ASTM D 4366, which records hardness by number of oscillation performed on surface of coating. Scratch resistance of coating panels was measured using scratch resistance tester (model 705) following ASTM D 7027. Samples were mounted on bed of the

equipment supported by platform for weight with scratching probe at an angle of 45° to the sample surface. The load at which the coating sustained and no damage is recorded was taken at scratch resistance. Impact strength of samples were measured using BYK-Gardener impact tester (model: IG-1120) following ASTM D 2794, a standard weight of 8 lb is dropped on steel coated panel from different heights. The highest value until no damage occurs was recorded as impact strength of the coating.

Differential scanning calorimetry (DSC) of epoxy/PANI modified formulations was studied using Q600, TA instruments to determine the effect of modification on glass transition temperature ( $T_g$ ) of coatings. The sample was placed in an aluminum pan and weighed. Finally, the sample was heated at 10 °C/min from 25 °C to 300 °C in a heating compartment under nitrogen environment.

Nano-indenter (Micro Materials, UK) was used to measure the indentation results such as hardness and elastic modulus for the conductive coatings. For this purpose a Berkovich type indenter was employed to test the coating surface using load control program. Nanoindentation tests were performed using load controlled program for our coating samples by providing maximum load of 250 mN. Where, the indenter was brought into the material at a constant strain rate of 10 s<sup>-1</sup> once the surface of the material was detected and until predefined maximum load was achieved. In order to determine the creep behavior, the applied load was held at its maximum for 60 s. The indenter was finally withdrawn from the surface at the same rate until the load is removed completely. At least 25 indentations were taken at different places to check the consistency in the results. All the calculations of results were performed by software because of known geometry.

The anticorrosive performance of epoxy coating system was investigated by the use of electrochemical impedance spectroscopy (EIS) measurements in a conventional three electrode cell with a three electrode; Ag/AgCl, stainless steel, and steel coated coupons were used as reference, counter and working electrodes, respectively. The area of the working electrode that was exposed to the test solution (3.5% NaCl solution) was of circa 10 cm<sup>2</sup>. EIS data were collected using an Autolab Ecochemie PGSTAT 30 (Potentiostat/Galvanostat) and the frequency scan was carried out by applying a ±5 mV amplitude sinusoidal wave perturbation at the corrosion potential value. The frequency range was scanned from 100 kHz to 1 mHz and the data were recording five impedance points per frequency.

### 3. RESULTS AND DISCUSSION

#### 3.1. Field emission scanning electron microscopy (FE-SEM)

Fig. 1 illustrates the SEM images of the modified epoxy coatings with (a) 0.16 wt. % PANI (b) 0.25 wt. % PANI (c) 0.63 wt. % PANI and (e) 0.78 wt. % PANI, respectively. The morphology of our coating system that was prepared using physical mixing technique shows that PANI particles are discretely distributed in the matrix of the epoxy and agrees with the work reported by Bluma et al. [12]. It is obviously noted from Fig. 1a that the distribution of particles in the lower percentages of PANI (EPANI1) is even and the sample possess a smooth surface. When the PANI concentration was increased in the epoxy coating (EPANI2), the distribution of PANI particles increased as shown in Fig. 1b. Further increases in the concentration of PANI in the epoxy matrix led to higher aggregation as can



be seen from Fig. 1c and Fig. 1d. This is most probably due to the poor interaction between PANI and the epoxy resin matrix at higher percentages as has been reported previously [13-14].

### 3.2. Mechanical properties

The effect of increasing PANI percentage on the mechanical properties of the manufactured epoxy coatings was studied using Koenig Pendulum hardness, scratch resistance, and impact strength. Dry film thickness (DFT) of these coatings was measured with the help of Sheen Minitest 3100. Table 2 shows the parameters obtained from studying the mechanical properties of epoxy coatings with different percentages of PANI. The Koenig pendulum hardness was determined on glass panels coated with epoxy/PANI coatings with DFT of 60-80  $\mu\text{m}$ . As the percentage of PANI in epoxy matrix increases, the pendulum hardness of the coating decreases. The addition of PANI in epoxy matrix is thus reducing the surface hardness of coating samples [15].

Other coated steel panels were used to report the scratch resistance of the epoxy/PANI coatings with DFT of 60-80  $\mu\text{m}$ . The highest scratch resistance was obtained for formulation with minimum quantity of PANI, EPANI1. Increasing the PANI percentage reduced the scratch resistance of coatings and least scratch resistance was obtained for formulations modified with 0.78wt% PANI (EPANI4). The change of the impact strength values of coatings with increasing PANI percentage in epoxy matrix resin are also given in Table 2. It is noted from Table 2 that the impact strength of the coatings increases with increasing the quantity of PANI increases and the highest value was recorded for the EPANI3. The addition of an increased PANI concentration, 0.78wt. %, in the resin matrix did not induce any changes in the properties.

**Table 2.** Pendulum hardness, scratch resistance, and impact strength values of PANI modified epoxy coatings.

Sample	Dry film thickness (DFT) $\mu\text{m}$	Pendulum hardness	Scratch resistance (Kg)	Impact strength (in/lb)
EPANI1	60-80	116	8	88
EPANI2	60-80	80	7	112
EPANI3	60-80	63	6.5	120
EPANI4	60-80	57	6.5	112

### 3.3. Differential scanning calorimetry (DSC)

The curing process of the different epoxy formulations was investigated using DSC analysis. Fig. 2 represents the change of the heat flow with temperature (DSC) curves obtained for (1) PANI1, (2) PANI2, (3) PANI3, and (4) PANI4, respectively. Fig. 2 indicates that the recorded DSC thermograms pattern was similar for all the formulations, whether PANI is incorporated or not. The formulation glass transition temperature ( $T_g$ ) value obtained was approximately 60  $^{\circ}\text{C}$ , which was attributed to the diglycidyl ether of bisphenol-A molecules at room temperature curing. Addition of

PANI into the matrix did not add any changes in the value of  $T_g$  for the modified coatings, which means that addition of PANI did not alter the thermal properties of coatings [16-17]. This was confirmed by the data listed in Table 3, which shows the effect of increasing PANI percentage on the change of  $T_g$  ( $^{\circ}\text{C}$ ) and indicates that the recorded  $T_g$  values were almost the same for both PANI free and PANI incorporated samples.

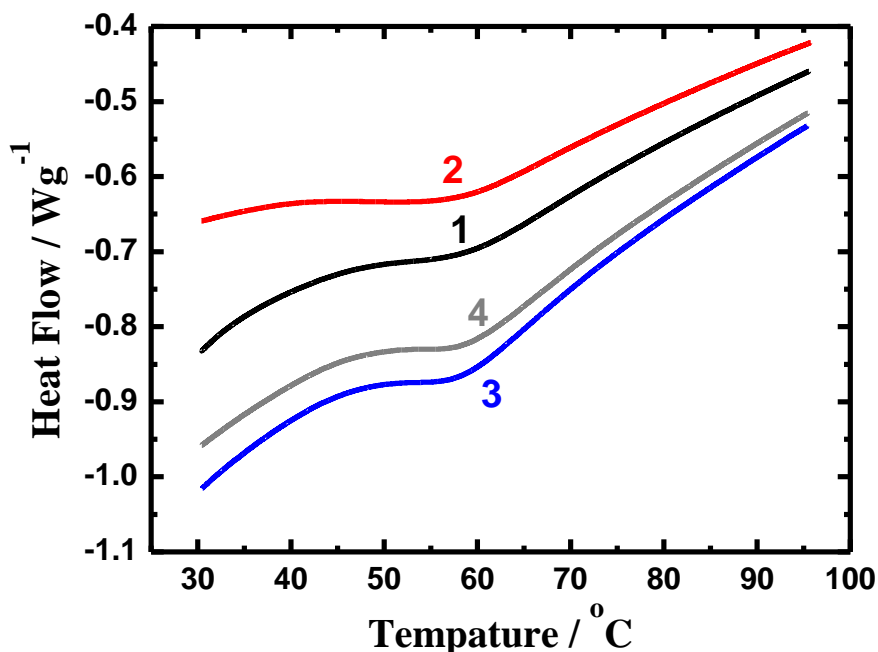


**Figure 2.** Change of the heat flow with temperature curves obtained for (1) EPANI1, (2) EPANI2, (3) EPANI3, and (4) EPANI4, respectively.

**Table 3.** DSC Analysis of the PANI modified formulations.

Sample	$T_g$ $^{\circ}\text{C}$
EPANI1	59.65
EPANI2	59.02
EPANI3	59.13
EPANI4	59.45

### 3.4. Nanoindentation investigation

Fig. 3 shows the typical loading followed by holding and then unloading profiles obtained for (a) EPANI1, (b) EPANI2, (c) EPANI3, and (d) EPANI4, respectively at maximum load of 250 mN. It is shown from Fig. 3 that the incorporation of PANI in the epoxy matrix generally increases the resistance against indentation force. Where, the increase of PANI content in the epoxy led to moving the curves of load vs. displacement towards the lower depth values. This confirms that the load bearing capacity of coating is increased, which agrees with the reported work by Armelin et al., [18]. It is also

seen that the sample with 0.25 wt. % PANI (EPANI2, Fig. 3b) exhibits the lowest depth penetration compared to the other modified coating samples. As the concentration of PANI increases, the gradient of load vs displacement graph at initial portion of unloading was also noted to be increased [19].

The effect of incorporating PANI on (a) the elastic modulus and (b) the indentation hardness obtained at 250 mN are shown respectively in Fig. 4. The behavior shown in Fig. 4a resembles to the stiffness of the material and additional to modulus of elasticity of the materials. Thus, a change in elastic modulus and hardness was expected accordingly by varying the percentage of PANI in epoxy matrix. The indentation modulus of the epoxy coatings was improved with the presence of the incorporated PANI content. Although, the presence of PANI significantly increases the modulus but the increase of its percentages leads to a slight change in the properties of coatings. It can be also seen from Fig. 4b that the hardness of PANI incorporated epoxy coatings was highly improved. Here, the hardness value increased significantly by adding 0.25 wt. % PANI (EPANI2) in compared to the epoxy without PANI, further addition of PANI in epoxy did not affect the hardness.

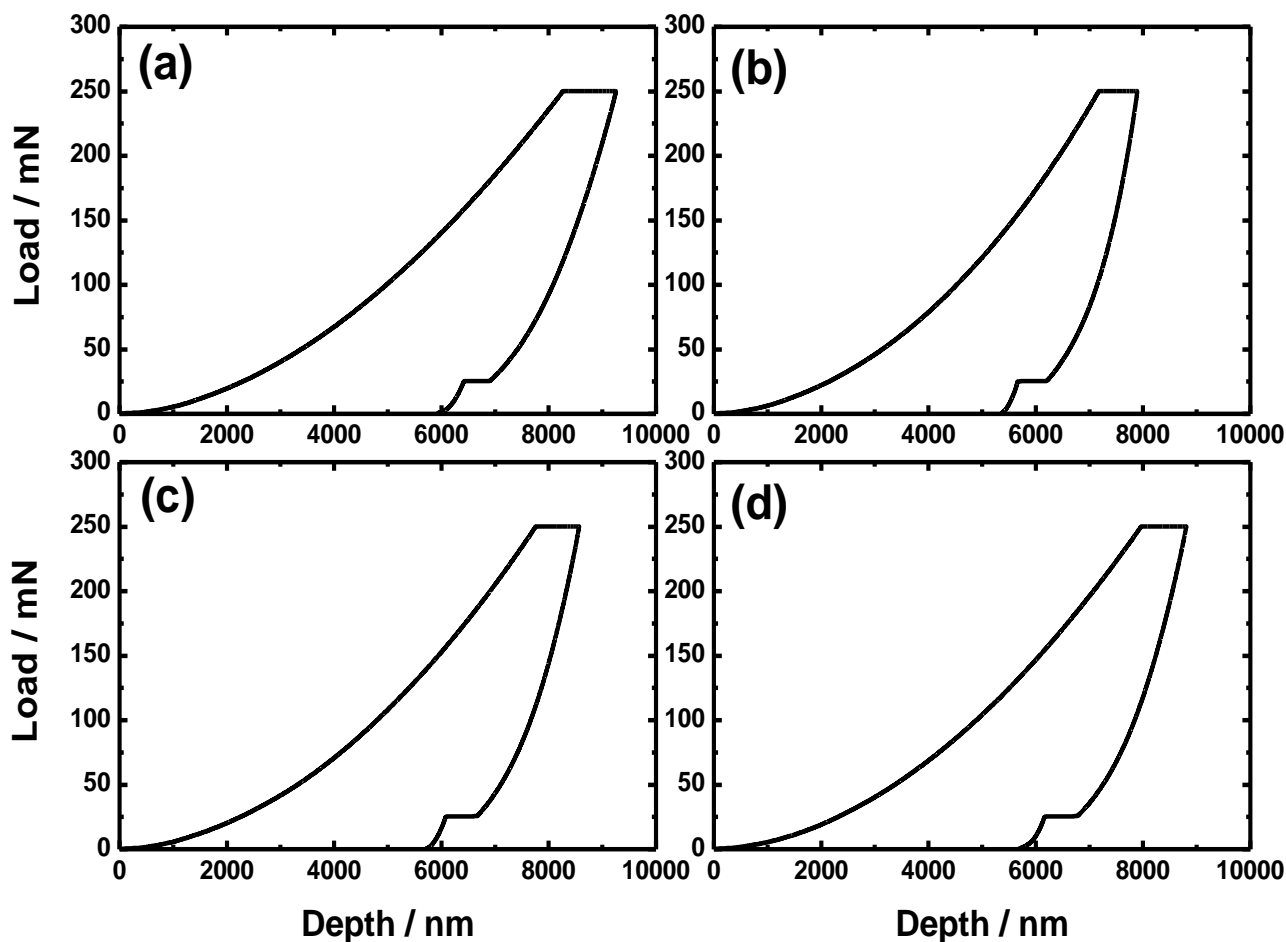


**Figure 3.** The nanoindentation Load vs. depth curves obtained for (a) EPANI1, (b) EPANI2, (c) EPANI3, and (d) EPANI4, respectively.



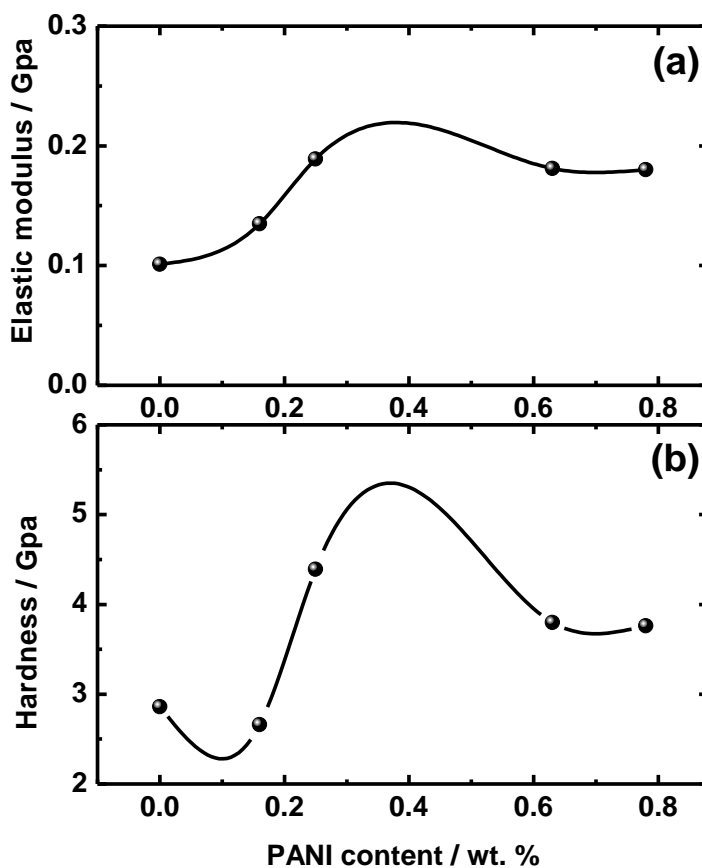


**Figure 4.** Effect of increasing PANI percentage on (a) elastic modulus and (b) hardness of the manufactured epoxy coatings.

As compared to the epoxy without PANI present, the increase in hardness was approximately 46% (from 0.101 GPa to 0.189 GPa) at 0.25 wt. % of PANI. However, the highest values of both hardness and modulus were achieved at 0.25 wt. % PANI addition. This results from the dispersion status of the particles of PANI in the epoxy matrix.

### 3.5. Fourier-transform infrared spectroscopy with attenuated total reflectance (FTIR-ATR)

In order to shed more light on the dispersions of the epoxy resin and if homogeneous, the curing agent, and PANI and to characterize the compositions of the fabricated PANI epoxy coatings through identifying their functional groups, the FTIR-ATR investigations were carried out. For this objective the various epoxy coating formulations cured with hardener were applied on small glass plates in order to measure the FTIR-ATR spectra after a complete curing for one week. Fig. 5 shows the ATR-IR spectra obtained for (a) EPANI1, (b) EPANI2, (c) EPANI3, and (d) EPANI4, respectively. The spectra were collected at this wide wavenumber range to ensure the obtaining the reflectance for every spectrum appeared from the surface of the different epoxy formula.

These spectra of ATR clearly exhibits the curing mechanism of ring opening reaction before and after the cross linking. The cross-linker polyamido-amine adduct-3282 and DGEBA epoxy resin functional groups have been displayed in the spectra. It has been reported [20] that the chemical

structure of the bisphenol based epoxy resin-A (BBERA) molecule has different organic groups, such as  $-\text{CH}_3$ ,  $\equiv\text{C}-\text{O}-\text{C}\equiv$ , aromatic rings, etc. On the other hand, the combination of DGEBA and PANI with different stoichiometric variations have several organic groups of  $=\text{C}=\text{O}$ ,  $-\text{OH}$ ,  $-\text{NH}_2$ ,  $-\text{N}=\text{N}-$ , etc in its molecule, is probably a compound has the combination of all these groups. The spectra appear from Fig. 5 show different peaks, some of them are; 748, 880, 1037, 1107, 1182, 1245, 1457, 1510, 1609, 1645, 1708, 2870, 2926, 2962, and  $3374\text{ cm}^{-1}$ . The presence of the peaks at 1400-1000 region, 1510, and  $1609\text{ cm}^{-1}$  has been reported [21-23] to be due to the presence of aromatic rings. Also, the appearance of the bands at 768 and  $827\text{ cm}^{-1}$  refer to the C-H out-of-plane deformation vibration bands due to the ring vibrations [20-24]. FTIR-ATR absorption spectra of the modified formulations were almost similar to the ones of the starting coatings. This means that there was no change in the epoxy-based resin resulted from the addition of the PANI's little concentrations. The structural characteristics of PANI products through FTIR-ATR [24] confirmed our data and indicated clearly that the consistent and homogenous peak distributions with the epoxy resin and the hardener employed in this investigation.

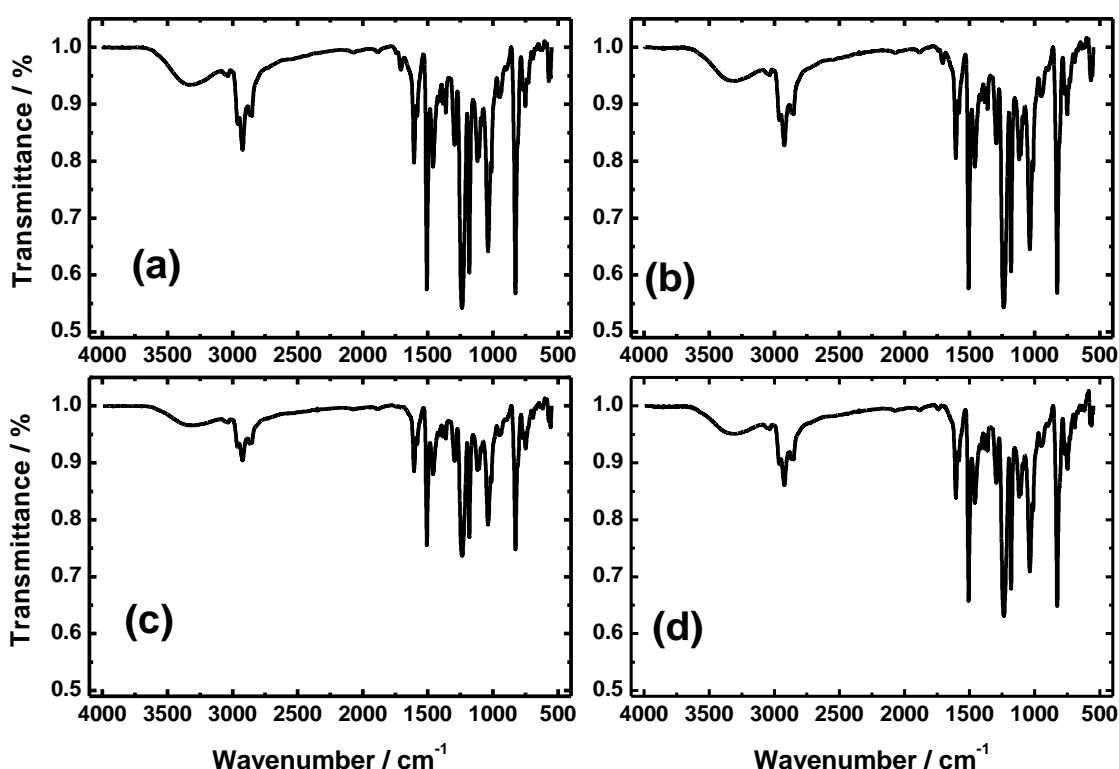


**Figure 5.** FTIR-ATR spectra obtained for (a) EPANI1, (b) EPANI2, (c) EPANI3, and (d) EPANI4, respectively.

### 3.6. Corrosion measurements using electrochemical impedance spectroscopy (EIS) technique

Our EIS measurements were carried out to report the kinetic parameters for the coated steel coupons and the test chloride solution after varied exposure intervals. Typical Nyquist plots obtained for EPANI1, (b) EPANI2, (c) EPANI3, and (d) EPANI4 after their immersion in 3.5% NaCl solutions

for 1 h are shown, respectively in Fig. 6. Similar EIS experiments were also performed for the different coatings in the sodium chloride solutions after 7 days and 21 days and the plots are shown in Fig. 7 and Fig. 8, respectively. The equivalent circuit model used to fit the experimental data shown in Fig. 6, Fig. 7, and Fig. 8 for the different coatings in the chloride solution is shown in Fig. 9. Table 4 lists the values of the parameters obtained from the fitting of the equivalent circuit. The symbols of these EIS parameters can be defined as following;  $R_S$  is the solution resistance, Q1 and Q2 are the constant phase elements (CPEs),  $R_{P1}$  and  $R_{P2}$  are the polarization resistances.

The Nyquist spectra show that the coated steel electrodes have a single semicircle followed by a segment as for 1 h (Fig. 6) and 7 days (Fig. 7) immersion in the test solution or even with increasing the time of immersion to 21 days (Fig. 8). Here, the big diameter of the semicircle and the large segment indicate that corrosion resistance of the coating in the chloride test solution is high. It is obvious from the EIS plots that the shorter the immersion time (1 h, Fig. 6) the bigger is the diameter of the semicircle and the larger is the obtained segment for all PANI incorporated epoxy coatings. The corrosion behavior over the short immersion period (1 h) reveals that the manufactured coatings had the ability to decrease the corrosion of the coated steel substrate due to the increase of their compactness of the coating layers.

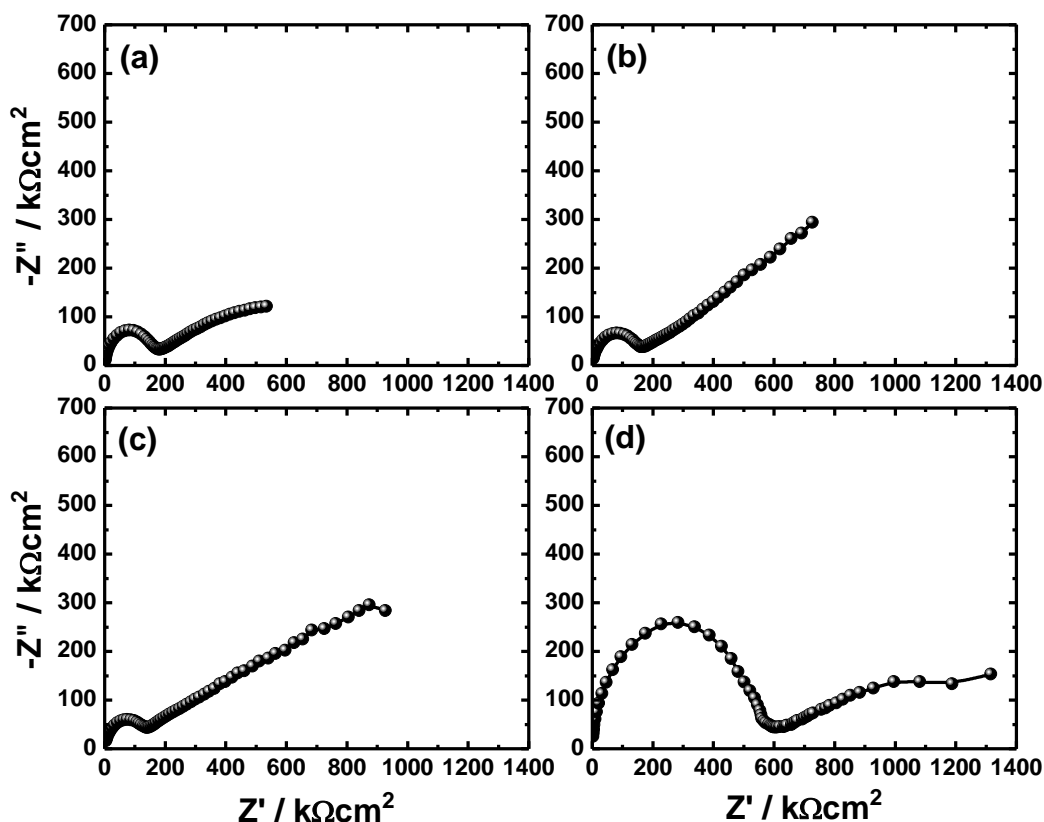


**Figure 6.** Typical Nyquist plots obtained for (a) EPANI1, (b) EPANI2, (c) EPANI3, and (d) EPANI4, respectively after their immersion in 3.5% NaCl solutions for 1 h.

The biggest semicircle diameter accompanied by the longest segment was noticed to be recorded for the EPANI4 (Fig. 6d), which had the highest PANI addition and indicates that the corrosion resistance of the epoxy coatings increases with the increase of PANI content.

Fig. 7 shows that increasing the time of immersion from 1 h to 7 days reduced the diameter of the semicircles and shortened the accompanied segment of passivation. Further increasing the immersion time to 21 days (Fig. 8) provided further decreasing in the diameter of the obtained semicircle with shorter passivation segment. It is clearly noted that the increase of the exposure period of time to 7 days and further to 21 days increased the corrosion of the coated coupons, which means that the corrosion resistance decreases with time. This was happening as a result of the degradation of the coating layers with increasing the immersion time. The degradation of coatings is most probably took place due to the presence of nonreacted epoxide groups that still present in the system [25], and the hydrolytic degradation can be responsible for the breakdown of etheric linkages causing electrolyte diffusion. On the other hand, Liu et al. [26] have claimed that coatings degrade as a result of the presence of the corrosive chloride ions, which leads to its diffusin into the coating/metal interface and attack the metal surface causing its corrosion.

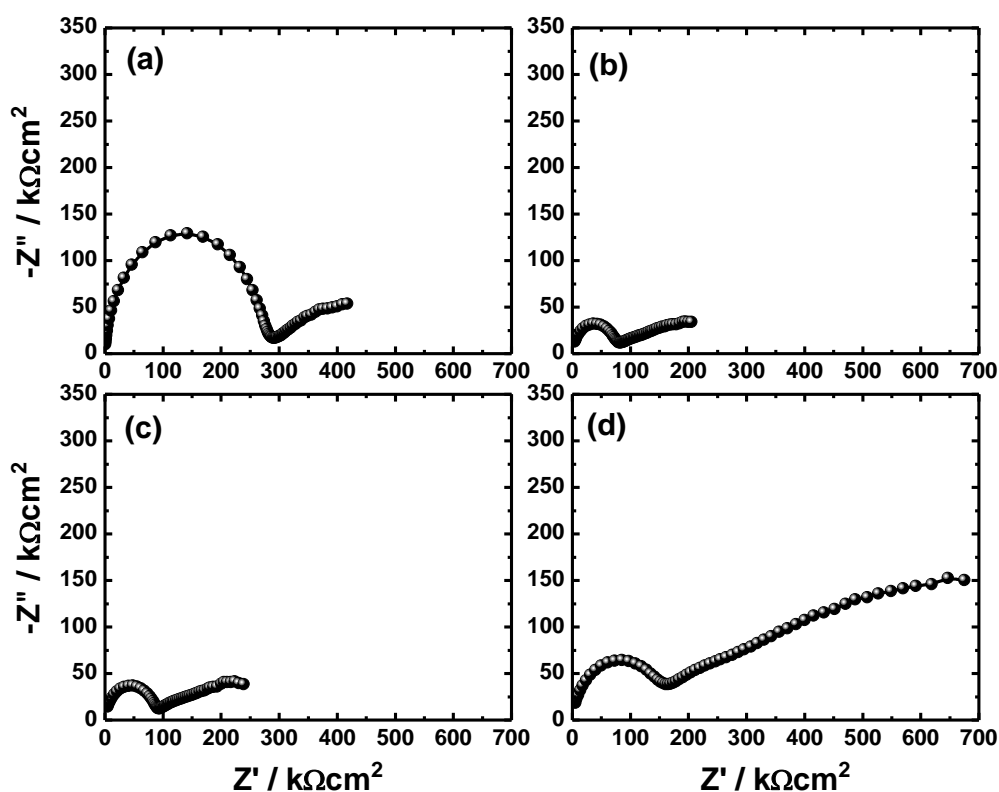


**Figure 7.** Typical Nyquist plots obtained for (a) EPANI1, (b) EPANI2, (c) EPANI3, and (d) EPANI4, respectively after their immersion in 3.5% NaCl solutions for 7 days.

The Nyquist spectra thus indicated that the best performance was recorded for the epoxy coating that had the highest PANI contents, 0.78 wt. %, which confirms that the increase of the PANI content leads to the increase of the corrosion resistance of the PANI incorporated coatings. This was also confirmed by the EIS parameters listed in Table 4, where the values of  $R_s$ ,  $R_{P1}$  and  $R_{P2}$  recorded higher values for all the epoxy coatings but the highest values were assigned for EPANI4. In addition,

the CPEs, Q1 with its n values close to unity represent double layer capacitors with some pores; the CPEs decrease upon the increase of PANI content, which are expected to cover the charged surfaces reducing the capacitive effects. Depending on the value of the “n” component, the CPEs, Q2, appear to have Warburg characters because the “n” values close to 0.5. This means that the mass transport is limited by the surface passive film due to the Warburg (W) characters.

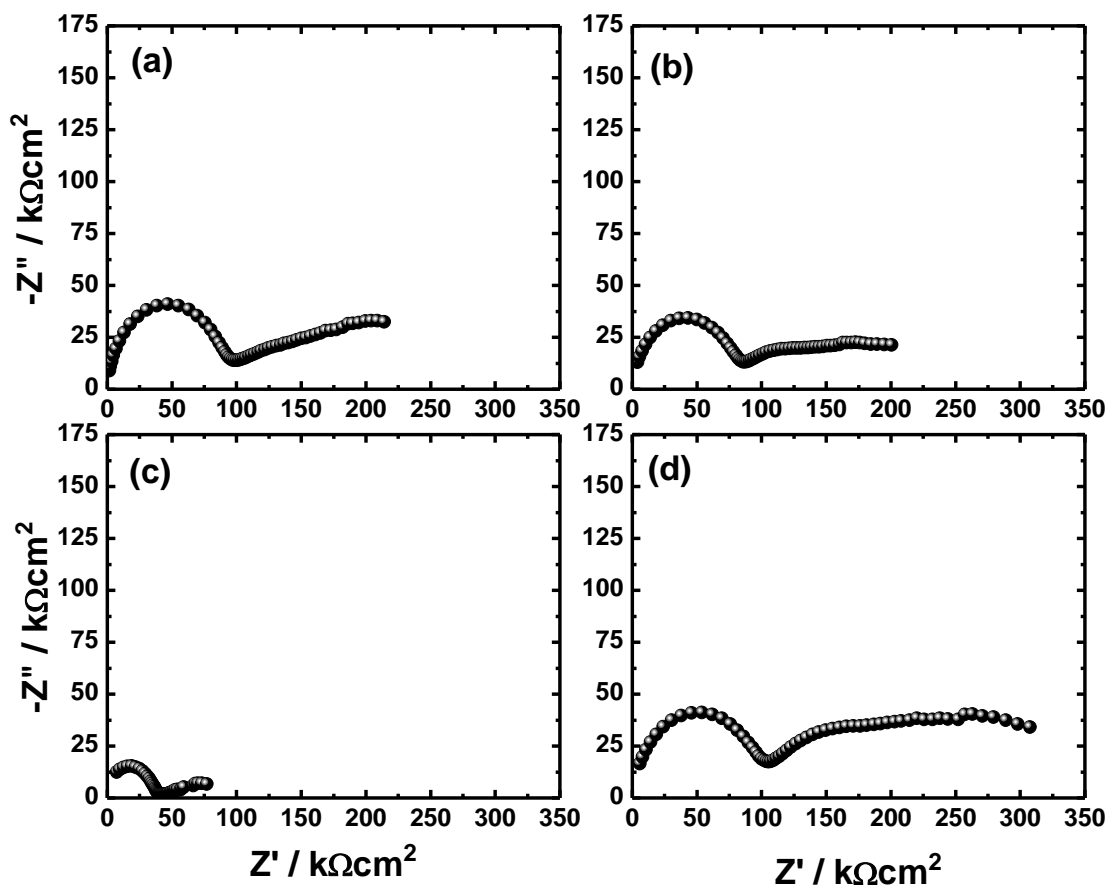


**Figure 8.** Typical Nyquist plots obtained for (a) EPANI1, (b) EPANI2, (c) EPANI3, and (d) EPANI4, respectively after their immersion in 3.5% NaCl solutions for 21 days.

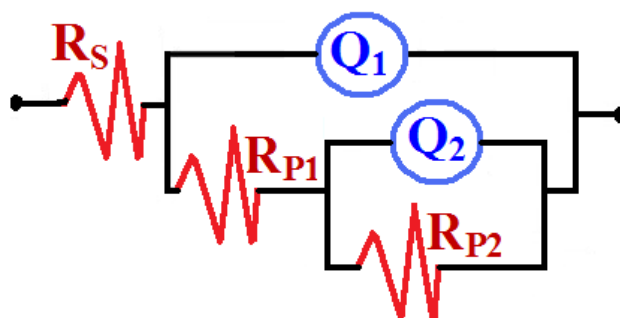


**Figure 9.** The equivalent circuit model used to fit the experimental data shown in Fig. 6, Fig. 7 and Fig. 8.

**Table 4.** EIS parameters obtained by fitting the Nyquist plots shown in Fig. 6, Fig. 7, and Fig. 8 with the equivalent circuit shown in Fig. 9 for the different PANI incorporated epoxy coatings immersed in 3.5% NaCl solutions for 1h, 7 days and 21 days, respectively.

Sample	Parameters						
	$R_s / \Omega \text{ cm}^2$	Q1		$R_{p1} / \text{k}\Omega \text{ cm}^2$	Q2		$R_{p2} / \text{k}\Omega \text{ cm}^2$
		$Y_Q / \text{nF cm}^{-2}$	n		$Y_Q / \mu\text{F cm}^{-2}$	n	
EPANI1 (1h)	199	3.16	0.93	145	3.62	0.35	861
EPANI2 (1h)	55.1	2.75	0.92	120	3.23	0.28	55100
EPANI3 (1h)	326	1.45	0.96	83.0	1.93	0.29	3700
EPANI4 (1h)	219	0.814	0.95	475	3.20	0.19	16100
EPANI1 (7d)	289	4.45	0.94	161	6.56	0.36	353
EPANI2 (7d)	13.1	2.78	0.92	64.7	8.47	0.28	304
EPANI3 (7d)	327	2.64	0.91	75.7	7.51	0.31	314
EPANI4 (7d)	41.1	2.13	0.91	119	2.35	0.31	1180
EPANI1 (21d)	47.8	3.26	0.94	80.4	8.10	0.30	254
EPANI2 (21d)	52.5	2.11	0.94	58.1	6.09	0.25	233
EPANI3 (21d)	105	2.73	0.90	29.3	44.1	0.12	67.3
EPANI4 (21d)	288	2.34	0.91	86.4	3.74	0.38	276

#### 4. CONCLUSIONS

Four epoxy coatings containing 0.16, 0.25, 0.63, and 0.78 wt. % PANI were synthesized by mechanical and sonication techniques. The FTIR-ATR spectra taken for the epoxy incorporated coatings have proven their chemical compositions. The FE-SEM images for the different coatings indicated that the coatings had homogenous dispersion of the PANI with epoxy resin. The mechanical properties of the different coatings were evaluated using hardness, scratch resistance, impact strength, nanoindentation, and thermal degradation testing methods. The mechanical tests indicated that the pendulum hardness and scratch resistance for the fabricated coatings slightly decrease, while the impact strength and corrosion resistance increase with the increase of PANI content. In addition to that the corrosion resistance of all coatings was tested in 3.5 wt. % NaCl solution for 1 h, 7 days, and 21 days using the EIS measurements. It has been found that the values of  $R_s$  and  $R_p$  resistances increase with increasing PANI content after all the examined exposure periods of time. Also, the increase of immersion time decreases the corrosion resistance due to the degradation of coatings, which is due to the chloride ions diffusion into the coating/metal interface and attack the metal surface. This effect increases with the increase of the time of immersion. Results together proved that the presence and the increase of PANI content highly improves the corrosion resistance of epoxy coatings.

#### ACKNOWLEDGEMENTS

The authors would like to thank the Center of Excellence for Research in Engineering Materials (CEREM), Advanced Manufacturing Institute (AMI), King Saud University and Saudi Arabian Oil Company (ARACMO) for financially supporting this work.



## References

1. D.W. DeBerry, *J. Electrochem. Soc.*, 132 (1985) 1022.
2. S. Koul, R. Chandra, S.K. Dhawan, *Polymer*, 41 (2000) 9305.
3. G. Mengoli, M.T. Munari, P. Bianco, M.M. Musiani, *J. Appl. Polym. Sci.*, 26 (1981) 4247.
4. M. Glatthaar, M. Niggemann, B. Zimmermann, P. Lewer, M. Riede, A. Hinsch, J. Luther, *Thin Solid Films*, 491 (2005) 298.
5. G.M. Spinks, A.J. Dominis, G.G. Wallace, D.E. Tallman, *J. Solid State Electrochem.*, 6 (2002) 85.
6. R.H. Baughman, *Synth. Met.*, 78 (1996) 339.
7. C. Ponce de León, S.A. Campbell, J.R. Smith and F.C. Walsh, *Trans. Inst. Metal Fin.*, 86 (2008) 34.
8. E. Armelin, R. Oliver, F. Liesa, J.I. Iribarren, F. Estrany and C. Alema'n, *Prog. Org. Coat.*, 59 (2007) 46.
9. S. Sathiyarayanan, S.S. Azim and G. Venkatachari, *Electrochim. Acta*, 52 (2007) 2068.
10. W.-K. Lu, S. Basak and R.L. Elsenbaumer: in 'Handbook of conductive polymers', (eds. T.A. Skotheim et al.), New York, Marcel Dekker (1997) pp. 881.
11. I. Jo, *Surf. Eng.*, 17 (2001) 265.
12. G.S. Bluma, L.C. Micheli, M. Magioli, X.M. Viviane, K. Dipak, *Synthetic Met.* 160 (2010) 1981.
13. S. P. Ali, C. Dehghanian, A. Kosari, *Corros. Sci.*, 85 (2014) 204.
14. M.R. Bagherzadeh, F. Mahdavi, M. Ghasemi, H. Shariatpanahi, H.R. Faridi, *Prog. Org. Coat.*, 68 (2010) 319.
15. A. Kalendová, D. Veselý, J. Stejskal, *Prog. Org. Coat.*, 62 (2008) 105.
16. R. Khan, U.A. Samad, M.A. Alam, M. Boumaza, S.M. Al-Zahrani, *Int. J. Advnc. Comp. Sci. Tech.* 2 (2013) 25.
17. L. Shen, L. Wang, T. Liu, H. Chaobin, *Macromol. Mater. Eng.*, 291 (2006) 1358.
18. E. Armelin, Á. Meneguzzi, A. F. Carlos, A. Carlos, *Surf. Coat. Tech.*, 203 (2009) 3763.
19. Y. WANG and X. JING, *Polym. J.*, 36 (2004) 374.
20. M. A. Alam, El-Sayed M. Sherif, S. M. Al-Zahrani, *Int. J. Electrochem. Sci.* 8 (2013) 3121.
21. N. B. Colthup, L. H. Daly, S. E. Wiberley, *Introduction to Infrared and Raman Spectroscopy*, 3rd ed., Academic Press, San Diego, CA, 1990.
22. G. Socrates, *Infrared Characteristic Group Frequencies Tables and Charts*, 3<sup>rd</sup> ed., Wiley & Sons Inc., New York, 2004.
23. El-Sayed M. Sherif, *Int. J. Electrochem. Sci.* 6 (2011) 3077.
24. B. Wetzell, F. Hauptert, M. Qiu Zhang, *Composite Sci. Technol.*, 63 (2003) 2055.
25. B. Ramezanzadeh, M.M. Attar, *Prog. Org. Coat.*, 71 (2011) 314.
26. J. Liu, F. Wang, K. C. Park, *Mater. Corros.*, 61 (2010) 9999.

© 2015 The Authors. Published by ESG ([www.electrochemsci.org](http://www.electrochemsci.org)). This article is an open access article distributed under the terms and conditions of the Creative Commons Attribution license (<http://creativecommons.org/licenses/by/4.0/>).